Mechanically exfoliated black phosphorus as a new saturable absorber for both Q-switching and mode-locking laser operation

Yu Chen,[1] Guobao Jiang,[2] Shuqing Chen,[2] Zhinan Guo,[1] Xuefeng Yu,[3] Chujun Zhao,[1,2] Han Zhang,[1,*] Qiaoliang Bao,[5] Shuangchun Wen,[2] Dingyuan Tang,[4] and Dianyuan Fan[1]

[1]*SZU-NUS Collaborative Innovation Centre for Optoelectronic Science & Technology, and Key Laboratory of Optoelectronic Devices and Systems of Ministry of Education and Guangdong Province, Shenzhen University, Shenzhen, China*

[2]*Key Laboratory for Micro-Nano Optoelectronic Devices of Ministry of Education, School of Physics and Electronics, Hunan University, Changsha 410082, China*

[3]*Institute of Biomedicine and Biotechnology, Shenzhen Institutes of Advanced Technology, Chinese Academy of Sciences, Shenzhen 518055, China*

[4]*School of Electrical and Electronic Engineering, Nanyang Technological University, Singapore 639798, Singapore*

[5]*Institute of Functional Nano and Soft Materials (FUNSOM), Jiangsu Key Laboratory for Carbon-Based Functional Materials and Devices, and Collaborative Innovation Center of Suzhou Nano Science and Technology, Soochow University, Suzhou 215123, China*

[*]*hzhang@szu.edu.cn*

Abstract: Black phosphorus (BP), an emerging narrow direct band-gap two-dimensional (2D) layered material that can fill the gap between the semi-metallic graphene and the wide-bandgap transition metal dichalcogenides (TMDs), had been experimentally found to exhibit the saturation of optical absorption if under strong light illumination. By taking advantage of this saturable absorption property, we could fabricate a new type of optical saturable absorber (SA) based on mechanically exfoliated BPs, and further demonstrate the applications for ultra-fast laser photonics. Based on the balanced synchronous twin-detector measurement method, we have characterized the saturable absorption property of the fabricated BP-SAs at the telecommunication band. By incorporating the BP-based SAs device into the all-fiber Erbium-doped fiber laser cavities, we are able to obtain either the passive Q-switching (with maximum pulse energy of 94.3 nJ) or the passive mode-locking operation (with pulse duration down to 946 fs). Our results show that BP could also be developed as an effective SA for pulsed fiber or solid-state lasers.

OCIS codes: (140.3510) Lasers, fiber; (140.4050) Mode-locked lasers; (140.3540) Lasers, Q-switched; (160.4330) Nonlinear optical materials.

References and links

1. D. A. Stetser and A. J. DeMaria, "Optical spectra of ultrashort optical pulses generated by mode-locked glass: Nd laser," Appl. Phys. Lett. **9**(3), 118–120 (1966).
2. V. N. Filippov, A. N. Starodumov, and A. V. Kir'yanov, "All-fiber passively Q-switched low-threshold erbium laser," Opt. Lett. **26**(6), 343–345 (2001).
3. L. Pan, I. Utkin, and R. Fedosejevs, "Passively Q-switched ytterbiumdoped double-clad fiber laser with a Cr^{4+}: YAG saturable absorber," IEEE Photon. Technol. Lett. **19**(24), 1979–1981 (2007).
4. S. Schön, M. Haiml, and U. Keller, "Ultrabroadband AIGaAs/CaF_2 semiconductor saturable absorber mirrors," Appl. Phys. Lett. **77**(6), 782–784 (2000).
5. L. A. Gomes, L. Orsila, T. Jouhti, and O. G. Okhotnikov, "Picosecond SESAM-based ytterbium mode-locked fiber lasers," IEEE J. Sel. Top. Quantum Electron. **10**(1), 129–136 (2004).
6. D. P. Zhou, L. Wei, B. Dong, and W. K. Liu, "Tunable passively Q-switched erbium-doped fiber laser with carbon nanotubes as a saturable absorber," IEEE Photon. Technol. Lett. **22**(1), 9–11 (2010).
7. B. Dong, C. Y. Liaw, J. Z. Hao, and J. H. Hu, "Nanotube Q-switched low-threshold linear cavity tunable erbium-doped fiber laser," Appl. Opt. **49**(31), 5989–5992 (2010).

#235000 - $15.00 USD Received 23 Feb 2015; revised 25 Apr 2015; accepted 27 Apr 2015; published 7 May 2015

8. M. Xu, T. Liang, M. Shi, and H. Chen, "Graphene-like two-dimensional materials," Chem. Rev. **113**(5), 3766–3798 (2013).
9. Q. H. Wang, K. Kalantar-Zadeh, A. Kis, J. N. Coleman, and M. S. Strano, "Electronics and optoelectronics of two-dimensional transition metal dichalcogenides," Nat. Nanotechnol. **7**(11), 699–712 (2012).
10. D. Popa, Z. P. Sun, T. Hasan, F. Torrisi, F. Wang, and A. C. Ferrari, "Graphene Q-switched, tunable fiber laser," Appl. Phys. Lett. **98**(7), 073106 (2011).
11. H. Kim, J. Cho, S. Y. Jang, and Y. W. Song, "Deformation-immunized optical deposition of graphene for ultrafast pulsed lasers," Appl. Phys. Lett. **98**(2), 021104 (2011).
12. A. Martinez, K. Fuse, and S. Yamashita, "Mechanical exfoliation of graphene for the passive mode-locking of fiber lasers," Appl. Phys. Lett. **99**(12), 121107 (2011).
13. Z. Luo, M. Zhou, J. Weng, G. Huang, H. Xu, C. Ye, and Z. Cai, "Graphene-based passively Q-switched dual-wavelength erbium-doped fiber laser," Opt. Lett. **35**(21), 3709–3711 (2010).
14. J. Du, Q. Wang, G. Jiang, C. Xu, C. Zhao, Y. Xiang, Y. Chen, S. Wen, and H. Zhang, "Ytterbium-doped fiber laser passively mode locked by few-layer Molybdenum Disulfide (MoS_2) saturable absorber functioned with evanescent field interaction," Sci. Rep. **4**, 6346 (2014).
15. S. Wang, H. Yu, H. Zhang, A. Wang, M. Zhao, Y. Chen, L. Mei, and J. Wang, "Broadband few-layer MoS_2 saturable absorbers," Adv. Mater. **26**(21), 3538–3544 (2014).
16. H. Liu, A. P. Luo, F. Z. Wang, R. Tang, M. Liu, Z. C. Luo, W. C. Xu, C. J. Zhao, and H. Zhang, "Femtosecond pulse erbium-doped fiber laser by a few-layer $MoS_{(2)}$ saturable absorber," Opt. Lett. **39**(15), 4591–4594 (2014).
17. D. Mao, Y. Wang, C. Ma, L. Han, B. Jiang, X. Gan, S. Hua, W. Zhang, T. Mei, and J. Zhao, "WS_2 mode-locked ultrafast fiber laser," Sci. Rep. **5**, 7965 (2015).
18. P. Yan, A. Liu, Y. Chen, H. Chen, S. Ruan, C. Guo, S. Chen, I. L. Li, H. Yang, J. Hu, and G. Cao, "Microfiber - based WS_2-film saturable absorber for ultra-fast photonics," Opt. Mater. Express **5**(3), 479–489 (2015).
19. Y. L. Chen, J. G. Analytis, J. H. Chu, Z. K. Liu, S. K. Mo, X. L. Qi, H. J. Zhang, D. H. Lu, X. Dai, Z. Fang, S. C. Zhang, I. R. Fisher, Z. Hussain, and Z. X. Shen, "Experimental realization of a three-dimensional topological insulator, Bi_2Te_3.," Science **325**(5937), 178–181 (2009).
20. C. Zhao, H. Zhang, X. Qi, Y. Chen, Z. Wang, S. Wen, and D. Tang, "Ultra-short pulse generation by a topological insulator based saturable absorber," Appl. Phys. Lett. **101**(21), 211106 (2012).
21. M. Jung, J. Lee, J. Koo, J. Park, Y. W. Song, K. Lee, S. Lee, and J. H. Lee, "A femtosecond pulse fiber laser at 1935 nm using a bulk-structured Bi_2Te_3 topological insulator," Opt. Express **22**(7), 7865–7874 (2014).
22. Z. Luo, Y. Huang, J. Weng, H. Cheng, Z. Lin, B. Xu, Z. Cai, and H. Xu, "1.06 μm Q-switched ytterbium-doped fiber laser using few-layer topological insulator Bi_2Se_3 as a saturable absorber," Opt. Express **21**(24), 29516–29522 (2013).
23. H. Liu, X. W. Zheng, M. Liu, N. Zhao, A. P. Luo, Z. C. Luo, W. C. Xu, H. Zhang, C. J. Zhao, and S. C. Wen, "Femtosecond pulse generation from a topological insulator mode-locked fiber laser," Opt. Express **22**(6), 6868–6873 (2014).
24. H. O. H. Churchill and P. Jarillo-Herrero, "Two-dimensional crystals: phosphorus joins the family," Nat. Nanotechnol. **9**(5), 330–331 (2014).
25. L. Li, Y. Yu, G. J. Ye, Q. Ge, X. Ou, H. Wu, D. Feng, X. H. Chen, and Y. Zhang, "Black phosphorus field-effect transistors," Nat. Nanotechnol. **9**(5), 372–377 (2014).
26. S. P. Koenig, R. A. Doganov, H. Schmidt, A. H. Castro Neto, and B. Özyilmaz, "Electric field effect in ultrathin black phosphorus," Appl. Phys. Lett. **104**(10), 103106 (2014).
27. F. Xia, H. Wang, and Y. Jia, "Rediscovering black phosphorus as an anisotropic layered material for optoelectronics and electronics," Nat. Commun. **5**, 4458 (2014).
28. T. Hong, B. Chamlagain, W. Lin, H. J. Chuang, M. Pan, Z. Zhou, and Y. Q. Xu, "Polarized photocurrent response in black phosphorus field-effect transistors," Nanoscale **6**(15), 8978–8983 (2014).
29. A. N. Rudenko and M. I. Katsnelson, "Quasiparticle band structure and tight-binding model for single-and bilayer black phosphorus," Phys. Rev. B **89**(20), 201408 (2014).
30. V. Tran, R. Soklaski, Y. Liang, and L. Yang, "Layer-controlled band gap and anisotropic excitons in few-layer black phosphorus," Phys. Rev. B **89**(23), 235319 (2014).
31. S. B. Lu, L. L. Miao, Z. N. Guo, X. Qi, C. J. Zhao, H. Zhang, S. C. Wen, D. Y. Tang, and D. Y. Fan, "Broadband nonlinear optical response in multi-layer black phosphorus: an emerging infrared and mid-infrared optical material," Opt. Express **23**(9), 11183–11194 (2015).
32. A. Martinez, K. Fuse, and S. Yamashita, "Mechanical exfoliation of graphene for the passive mode-locking of fiber lasers," Appl. Phys. Lett. **99**(12), 121107 (2011).
33. Y. M. Chang, H. Kim, J. H. Lee, and Y. W. Song, "Multilayered graphene efficiently formed by mechanical exfoliation for nonlinear saturable absorbers in fiber mode-locked lasers," Appl. Phys. Lett. **97**(21), 211102 (2010).
34. J. Sotor, G. Sobon, W. Macherzynski, P. Paletko, K. Grodecki, and K. M. Abramski, "Mode-locking in Er-doped fiber laser based on mechanically exfoliated Sb_2Te_3 saturable absorber," Opt. Mater. Express **4**(1), 1–6 (2014).
35. M. Engel, M. Steiner, and P. Avouris, "Black phosphorus photodetector for multispectral, high-resolution imaging," Nano Lett. **14**(11), 6414–6417 (2014).
36. Y. Chen, C. Zhao, H. Huang, S. Chen, P. Tang, Z. Wang, S. Lu, H. Zhang, S. Wen, and D. Tang, "Self-assembled topological insulator-Bi_2Se_3 membrane as a passive Q-switcher in an erbium-doped fiber laser," J. Lightwave Technol. **31**(17), 2857–2863 (2013).

#235000 - $15.00 USD Received 23 Feb 2015; revised 25 Apr 2015; accepted 27 Apr 2015; published 7 May 2015

37. A. Castellanos-Gomez, L. Vicarelli, E. Prada, J. O. Island, K. L. Narasimha-Acharya, S. I. Blanter, D. J. Groenendijk, M. Buscema, G. A. Steele, J. V. Alvarez, H. W. Zandbergen, J. J. Palacios, and H. S. J. van der Zant, "Isolation and characterization of few-layer black phosphorus," 2D Mater. **1**(2), 025001 (2014).
38. H. Ahmad, M. Z. Zulkifli, F. D. Muhammad, A. Z. Zulkifli, and S. W. Harun, "Tunable graphene-based Q-switched erbium-doped fiber laser using fiber Bragg grating," J. Mod. Opt. **60**(3), 202–212 (2013).
39. T. Jiang, Y. Xu, Q. J. Tian, L. Liu, Z. Kang, R. Y. Yang, G. S. Qin, and W. P. Qin, "Passively Q-switching induced by gold nanocrystals," Appl. Phys. Lett. **101**(15), 151122 (2012).
40. Z. Yu, Y. Song, J. Tian, Z. Dou, H. Guoyu, K. Li, H. Li, and X. Zhang, "High-repetition-rate Q-switched fiber laser with high quality topological insulator Bi_2Se_3 film," Opt. Express **22**(10), 11508–11515 (2014).
41. H. Li, H. Xia, C. Lan, C. Li, X. Zhang, J. Li, and Y. Liu, "Passively Q-switched erbium-doped fiber laser based on few-layer MoS_2 saturable absorber," IEEE Photon. Technol. Lett. **27**(1), 69–72 (2015).
42. J. Kang, J. D. Wood, S. A. Wells, J. H. Lee, X. Liu, K. S. Chen, and M. C. Hersam, "Solvent exfoliation of electronic-grade, two-dimensional black phosphorus," ACS Nano **9**(4), 3596–3604 (2015).
43. W. Liu, C. Ren, H. Han, J. Tan, Y. Zou, X. Zhou, P. Huai, and H. Xu, "First-principles study of the effect of phosphorus on nickel grain boundary," J. Appl. Phys. **115**(4), 043706 (2014).
44. A. S. Rodin, A. Carvalho, and A. H. Castro Neto, "Strain-induced gap modification in black phosphorus," Phys. Rev. Lett. **112**(17), 176801 (2014).

1. Introduction

In order to achieve pulse emission of lasers, Q-switching and mode-locking based on saturable absorber (SA) are the widely used techniques due to the advantages of excellent mechanical stability, easy implementation and low cost. Since the first generation of SA when the Nd: glass laser was successfully used for pulse generation in 1966 [1], various type of SAs had been intensively investigate developed, such as the ion-doped crystals [2,3], Semiconductor Saturable Absorption mirror (SESAM) [4,5], and Carbon Nano-Tube (CNT) [6,7]. Among them, the SESAMs are the most widely used one due to their high flexibility and stability. However, SESAMs have the drawbacks of high cost and a limited range of optical response, which restrict their applications to a great extent. Strong aspiration of low-cost SAs with broadband operation has always been at the central issue of laser experts. Recently, originating from the intensive research enthusiasm of graphene, there have been tremendous advancements in the fields of photonics based on two dimensional (2D) materials based photonics [8]. The unique optoelectronic characteristics and the capability of being easily stacking towards multilayer hetero-structures of the materials had been proved to be able to produce novel and distinctive optoelectronic devices [9]. Graphene based SAs have been studied and developed. They have the advantages of ultra-fast recovery time and broadband saturable absorption [10–13]. But the absence of band-gap and the low absorption co-efficiency (2.3%/layer) of graphene have also restraint its applications in situations where strong light-matter interaction is required. Lately, transition-metal dichalcogenides (like molybdenum disulfide (MoS_2)) have attracted much attention of laser researches because of their thickness dependent band-gap and unique absorption property [14–16] (MoS_2: monolayer, direct band-gap of 1.8 eV; few-layers, indirect band-gap of 0.86–1.29 eV [15]). Besides MoS_2, very recently a series of MoS_2 like 2D semiconducting SAs, such as WS_2, VS_2 and $MoSe_2$, have also been extensively investigated as effective SAs for pulse laser applications [17,18]. Although by introducing some suitable defects transition-metal dichalcogenides could also be developed for IR and mid-IR optoelectronics, the preparation process might become extremely difficult. Another 2D material, topological insulator (TI), has insulating bulky states with indirect band-gap of 0.35 eV [19] and gapless surface states. It had also been successfully applied as an effective SA [20–23], but has again the drawback of complicated preparation process (compound with two different elements), which severely limited its applications in optoelectronic devices.

Currently, another rising 2D material: black phosphorus (BP)-the most thermo- dynamically stable allotrope of phosphorus, has attracted attention of researches [24]. There have been plenty interesting findings on its unique electronic properties [25,26], however, its optical properties are much less touched, except the polarization dependent optical response as determined by the anisotropic feature of BPs [27,28]. Different from the above-mentioned 2D

#235000 - $15.00 USD Received 23 Feb 2015; revised 25 Apr 2015; accepted 27 Apr 2015; published 7 May 2015

materials, BP has a layer-dependent direct band-gap: it changes from 0.35 eV (bulk) to 2 eV (monolayer layer) [29,30]. This makes BP to fill up the "blank space" between semi-metallic graphene and wide band-gap transition-metal dichalcogenides. Note that BP comprises only the elemental "phosphorus". Hence it could be easily peeled off by mechanical exfoliation. Stimulated by the similarity between graphene and BP in terms of single elemental component and direct band-gap, it is natural to find out whether BP could be used as a SA for the IR and mid-IR optoelectronics. The broadband nonlinear optics response of few layer BPs had been recently reported by our research group [31], while BP-based nonlinear optical devices were still untouched.

In this contribution, we have demonstrated the fabrication of BP 2D-material by the mechanical exfoliation method and the application of the 2D BP material as a new type of effective SA for ultra-fast photonics. Through mechanical exfoliation approach just by scotch tape, bulk BPs could be peeled into 2D thin layers, which could be attached onto the end-facet of a fiber ferrule, making it into a SA device. By placing such optical saturable absorber devices inside different Erbium-doped all-fiber laser cavities, either the passive Q-switching or mode locking operation of the fiber laser could be obtained, which therefore suggests that 2D BP material could be developed as an effective SA for ultra-fast photonics.

2. Preparation and characteristics of BP

In our experiments, the BP-SA was prepared by mechanical exfoliation method (showing in Fig. 1(a), the green layer is BP), which has been widely used in two-dimensional materials based ultra-fast fiber laser applications, such as graphene [32,33], and TIs [34]. For all-fiber-based applications, the key issue is how to transfer the mechanically exfoliated materials to the fiber end-facet. Mechanical exfoliation is advantageous mainly because of its simplicity and reliability, where the entire fabrication process is absent of any chemical procedures and costly instruments. As shown in Fig. 1(a), the relatively thin flakes were moderately peeled from a big block of commercial BP using scotch tape. Then, we repeatedly pressed the flakes adhered on the scotch tape so that the BP flakes become thin enough to transmit light through the BP flakes with high efficiency. In the following, we pushed down a fresh standard FC/PC fiber ending to the side with BP flakes. Owing to the strong adhesive force between BP and ceramic, thinner BP could be further attached onto the fiber end-facet. After connecting with another FC/PC fiber ferrule with a standard flange adapter, the all-fiber BP-SA was finally achieved. Raman spectrum of the mechanically exfoliated BP on the scotch tape was shown in Fig. 1(b). There are three distinct Raman peaks at 361 cm^{-1}, 438 cm^{-1} and 465 cm^{-1} [35], corresponding to the A_g^1, B_{2g} and A_g^2 vibration modes of layered BP. While the B_{2g} and A_g^2 modes correspond to the in-plane oscillation of phosphorus atoms in BP layer, and the A_g^1 modes corresponds to the out-of-plane vibration.

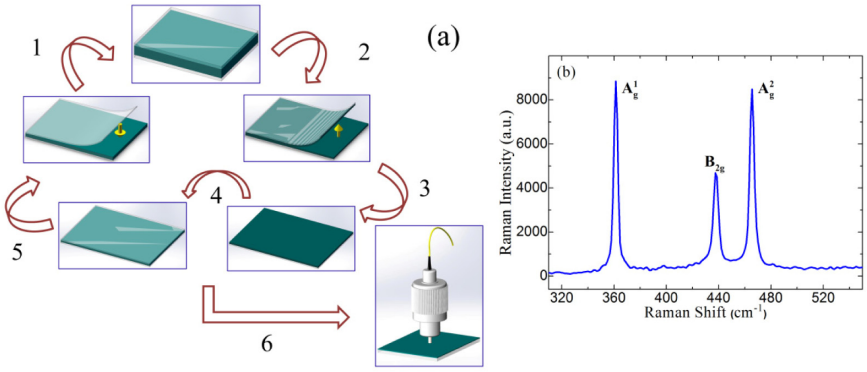

Fig. 1. (a) The process of mechanical exfoliation method. (b) Raman spectra of BP

#235000 - $15.00 USD Received 23 Feb 2015; revised 25 Apr 2015; accepted 27 Apr 2015; published 7 May 2015

BP-SAs had been prepared with different thicknesses. As shown in Figs. 2(a) and 2(b), the fiber core was almost entirely covered by the BP. We also characterized the nonlinear optical response of the BP-SAs using the balanced synchronous twin-detector measurement [36]. The corresponding curves are shown in Figs. 2(c) and 2(d). After fitting with formula: $T(I) = 1 - \Delta T * \exp(-I / I_{sat}) - T_{ns}$ ($T(I)$: transmission, ΔT: modulation depth, I: input intensity, I_{sat}: saturation power intensity, T_{ns}: non-saturable absorbance), we obtained the corresponding saturable absorption parameters. The modulation depth and saturation intensity of two BP-SAs are 18.55%, 10.74 MW/cm^2, and 8.1%, 6.55 MW/cm^2 respectively. Noting that the optical absorption in low power of relatively thick BP is about 65%, relatively thick BP about 38%, we estimate that the number of relatively thick BP is about 25 layers, and relatively thin BP is about 15 layers (the optical absorption of monolayer BP was estimated to 2.8% [37]).

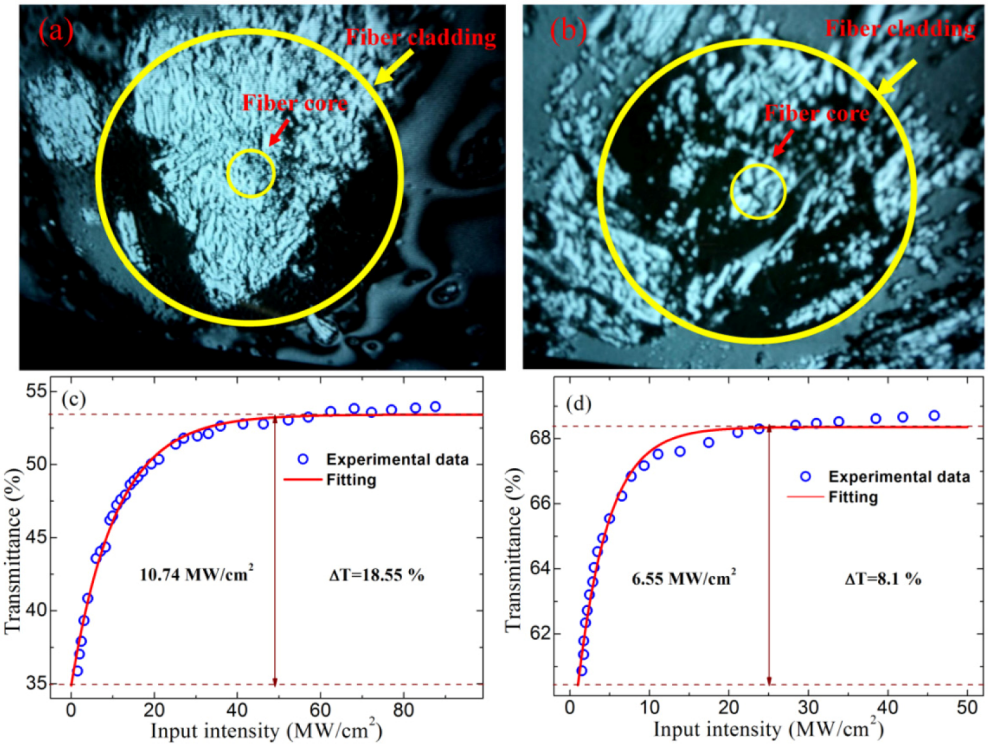

Fig. 2. Optical image of the fiber end-facet (fiber cladding diameter of 125 μm, fiber core diameter of 9 μm) covered with relatively thick (a) and thin (b) BP and the measured saturable absorption data and its corresponding fitting curve of relatively thick (c) and thin (d) BP

3. Fiber laser setup

To test the passively Q-switching and/or mode-locking ability of the BP-SAs, we constructed an erbium-doped fiber ring laser with a cavity configuration as shown in Fig. 3(a). The fiber laser cavity is made of the standard fiber-optic components such as wavelength division multiplexer (WDM), polarization controller (PC), coupler, optical isolator, erbium-doped fiber (EDF), and single mode fiber (SMF). The fiber laser operating in the anomalous dispersion regime has a ring cavity with a total length of 56.7 m, comprising a piece of 0.9 m erbium-doped fiber (EDF, LIEKKI Er 80-8/125) with a group velocity dispersion (GVD) parameter of 15.8 ps/nm/km and 55.8 m standard single mode fiber (SMF-28) with a GVD parameter of 18 ps/nm/km at 1550 nm. The pump from a 975 nm laser diode (LD) source is

#235000 - $15.00 USD Received 23 Feb 2015; revised 25 Apr 2015; accepted 27 Apr 2015; published 7 May 2015

coupled into the cavity through a 980/1550 wavelength-division multiplexer (WDM), and a 10% fiber coupler is employed to output the laser emission. A polarization independent isolator (PI-ISO) is used to force the unidirectional operation of the ring cavity, and a polarization controller (PC) is used to fine adjust the polarization state of circulating light and the cavity birefringence. An optical spectrum analyzer (Ando AQ-6317B) and a real time oscilloscope with a bandwidth of 4 GHz (Agilent DSO9404A) combined with a 5 GHz photo-detector (Thorlabs SIR5) are employed to simultaneously monitor the optical spectrum and the temporal evolution of the output pulse train. The crystal structure of BP is also provided in Figs. 3(c)–(e) with 3D view, lateral view and top view.

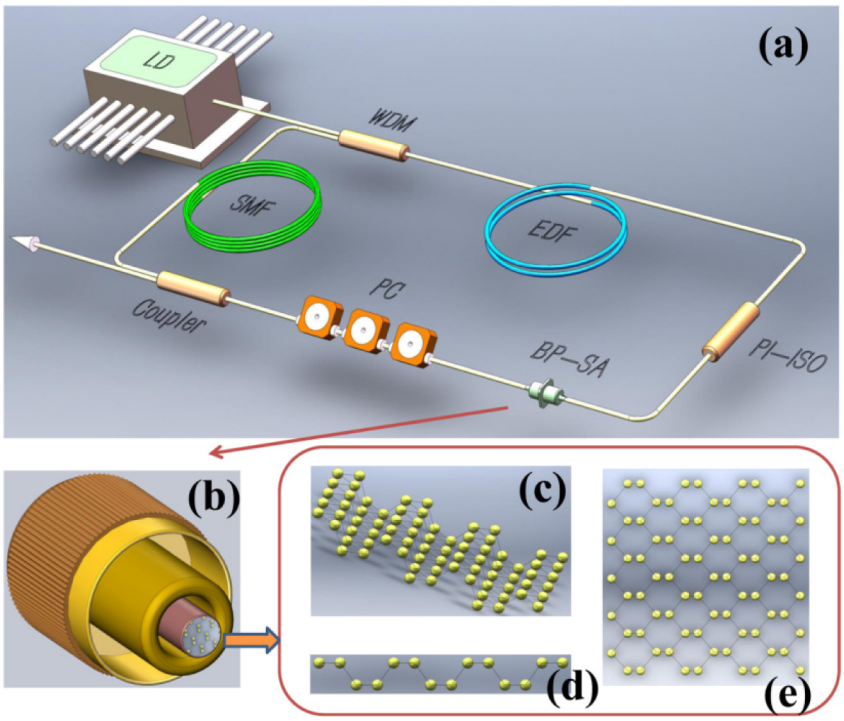

Fig. 3. (a) Experimental setup of the BP-SA based Q-switching Erbium-doped fiber laser.(b) The fiber ending coated by BP. The crystal structure of BP: (c) 3D view; (d) lateral view; (e) top view

4. Experimental results and discussions

Firstly, the BP-SA with a modulation depth of 18.55%, and saturation intensity of 10.74 MW/cm^2 was incorporated in the cavity. Self-started Q-switching state was obtained just by increasing the pump power up to 50 mW. For the laser, the oscillation threshold was 35 mW. Fig. 4 summarizes the typical characteristics of Q-switching state at a pump power of 110 mW. Fig. 4(a) shows the typical Q-switching pulse train. It has a repetition rate of 10.42 kHz, corresponding to a pulse interval of 95.97 μs. No peak intensity modulation had been found on pulse train, illustrating the high stability of Q-switching operation. The absence of Q-switching instability is further verified by the real-time recorded single pulse profiles. There were no top amplitude fluctuations, as shown in Fig. 4(b). It has a symmetric Gaussian-like shape with a full width at half maximum (FWHM) of 13.2 μs. The corresponding optical spectrum is shown in Fig. 4(c), from which we can infer that the 3 dB spectral bandwidth of the Q-switching output is about 0.2 nm centered at 1562.87 nm. To investigate the stability of this Q-switching fiber laser, we also measured the corresponding Radio Frequency (RF)

#235000 - $15.00 USD Received 23 Feb 2015; revised 25 Apr 2015; accepted 27 Apr 2015; published 7 May 2015

spectrum centered at 10.42 kHz, as shown in Fig. 4(d). The signal-to-noise ratio (SNR) is up to about 45 dB.

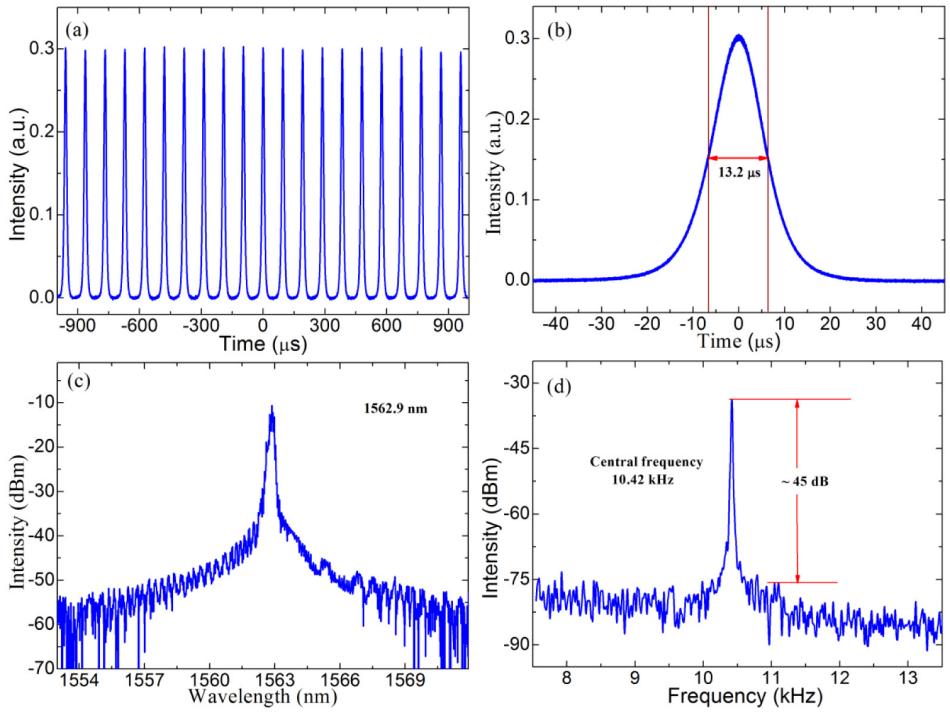

Fig. 4. Typical characteristics of Q-switching pulse emitted from our BP-SA-based fiber laser at pump power of 110 mW: (a) Output pulse train; (b) Single pulse profile; (c) optical spectrum; (d) corresponding RF spectrum

We experimentally investigated the evolution of the Q-switching pulse train with the pump power increase, as shown in Fig. 5. At the pump power of 50, 90, 130, 185 mW the pulse repetition rate was 6.893, 9.116, 11.92, 15.47 kHz, respectively. From which, it shows the feature of Q-switching that the pulse repetition gradually increases as the pump power increases. Noting that the output pulses trains were still kept stable with relatively uniform intensity distribution during the entire process of tuning the pump power, we can reasonably conclude that the fiber laser operates in highly stable Q-switching regime.

#235000 - $15.00 USD Received 23 Feb 2015; revised 25 Apr 2015; accepted 27 Apr 2015; published 7 May 2015

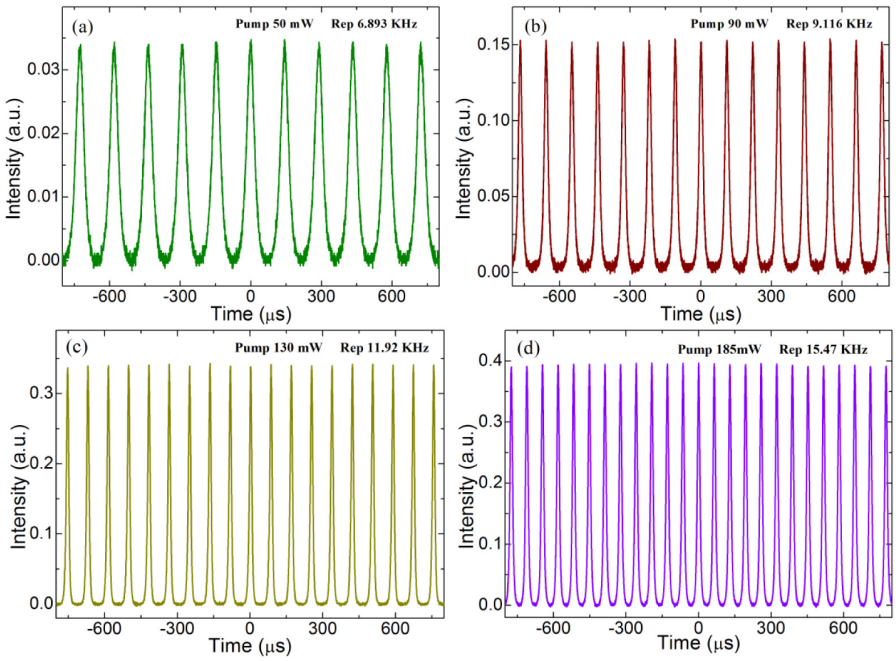

Fig. 5. Output pulse trains obtained at different pump powers

Fig. 6 shows the Q-switched pulse parameter variation with the pump power. Fig. 6(a) is the average output power and the pulse energy changes with the pump power. The average output power increased almost linearly with the pump power. Most importantly, at the maximum pump power of 195 mW the maximum obtained pulse energy is up to 94.3 nJ, which is comparable to those of the Q-switch pulses obtained in Er-doped fiber lasers with other SAs, such as CNT [7], Graphene [38], Gold nano-crystal [39], TI [36]. Once the pump power exceeded 180 mW, the Q-switching output became unstable where strong intensity modulation appeared. If the pump power was further boosted higher than 195 mW, the Q-switching state suddenly disappeared and a continuous wave (CW) state was obtained. The Q-switching state could be attained again just by decreasing the pump power. We explain this phenomenon as due to the over-saturation of the BP-SA rather than the thermal damage [40,41]. Fig. 6(b) demonstrates the evolution of the repetition rate and pulse duration with the pump power. It shows typical features of the Q-switching operation. With the increasing of the pump power, the repetition rate linearly increases from 6.983 kHz to 15.78 kHz, while the pulse duration varied in the range of 39.84 μs to 10.32 μs. In the low pump power regime, the pulse width decreases rapidly, most probably due to the fast accumulation of electrons in the upper energy level. However, in the high pump power regime, due to the over-saturation, the speed of accumulation slows down, leading to less significant change of pulse widths.

#235000 - $15.00 USD Received 23 Feb 2015; revised 25 Apr 2015; accepted 27 Apr 2015; published 7 May 2015

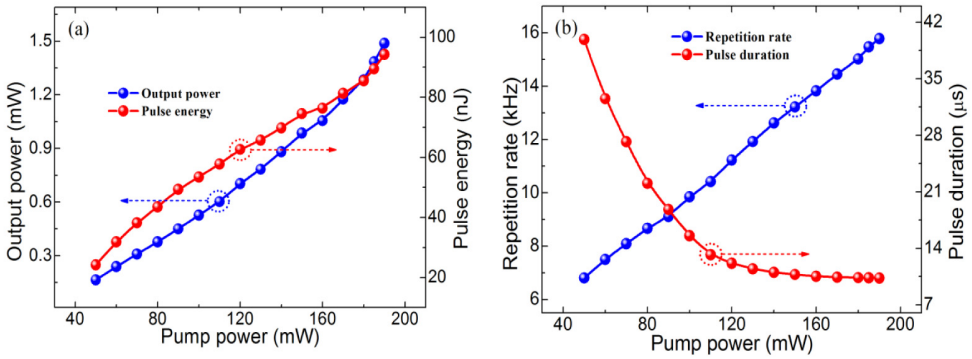

Fig. 6. The evolution of output average power and pulse energy (a), pulse repetition rate and duration and (b) as pump power increases

The operation (Q-switching or mode-locking) of fiber lasers strong depends on the saturable absorption parameters of SAs. There is a critical parameter: $E^2 = E_G E_{SA} \Delta T$, where E_G is gain saturation energy of the laser, E_{SA} and ΔT are the saturation energy and modulation depth of the SA, respectively. When the single pulse energy in the cavity E_p satisfies $E_p^2 > E^2$, the CW mode-locking can be obtained. Otherwise, the Q-switched mode-locking or Q-switching operation will be achieved. Therefore, in order to obtain mode-locking operation more easily, one should depress the value of E as much as possible. Obviously, E_G is fixed by the gain fiber, the only factor that can decrease E is be E_{SA} and ΔT .

We then incorporated another BP-based SA that has a modulation depth of 8.1% and a saturable intensity of 6.55 MW/cm^2 in the cavity. With a cavity length of 15 m, the self-started mode locking operation with a threshold pump of 63.7 mW was obtained. Fig. 7 summarizes the characteristics of the mode-locking operation of the fiber laser at pump power of 85.4 mW. Fig. 7(a) (down) shows the single pulse train recorded over 2 μs. The pulses have a repetition rate of 5.96 MHz, which matches well with the cavity length, indicating that the laser operates in the mode-locking state. Fig. 7(a) (up) shows the same pulse train but recorded over 40 μs, showing the high stability of the pulses as there is no pulse peak intensity modulation. The corresponding optical spectrum, as shown in Fig. 7(b), has obvious Kelly spectral sidebands, indicating that the fiber laser is operating in the soliton regime. It has a central wavelength of 1571.45 nm and a 3 dB bandwidth of 2.9 nm. Correspondingly, as shown in Fig. 7(d), the measured autocorrelation (AC) trace can be well fitted by the hyperbolic secant function with a full width at half maximum (FWHM) of 1.46 ps, indicating that the real pulse width is about 946 fs. The time-bandwidth product is 0.328, showing that the obtained soliton pulse is almost transform limited. Fig. 7(c) (the insert) is the corresponding RF spectrum with a resolution bandwidth (RBW) of 10 Hz. The signal-to-noise ratio (SNR) is up to 70 dB, which suggests that the fiber laser operates in a high stable regime. Moreover, the long scale RF spectrum shows no any extra frequency components except the fundamental and harmonic frequency components.

#235000 - $15.00 USD Received 23 Feb 2015; revised 25 Apr 2015; accepted 27 Apr 2015; published 7 May 2015

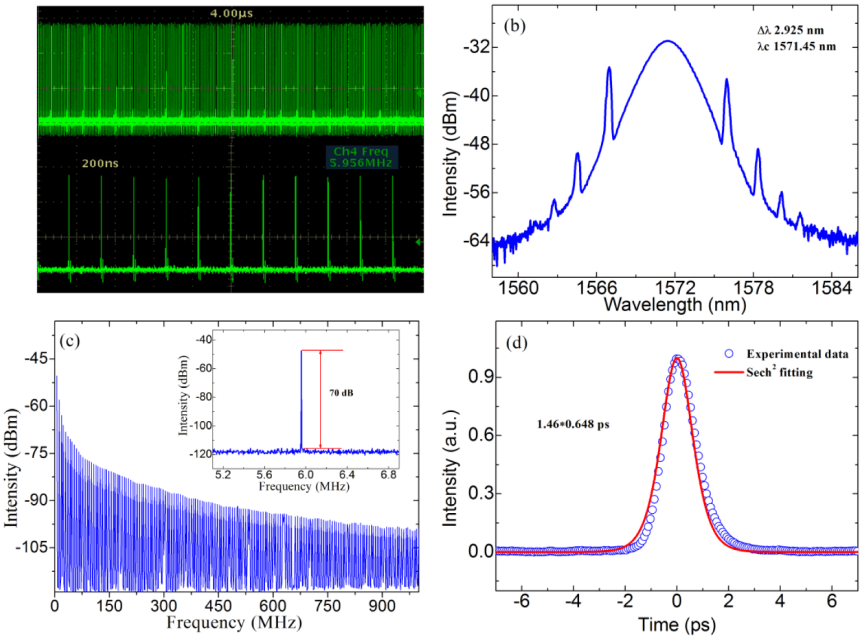

Fig. 7. Typical Mode-locking output: (a) Output pulse train; (b) the corresponding spectrum; (c) the measured autocorrelation trace and its fitting curve; (d) RF spectrum. Inset: RF spectrum in 1 GHz span

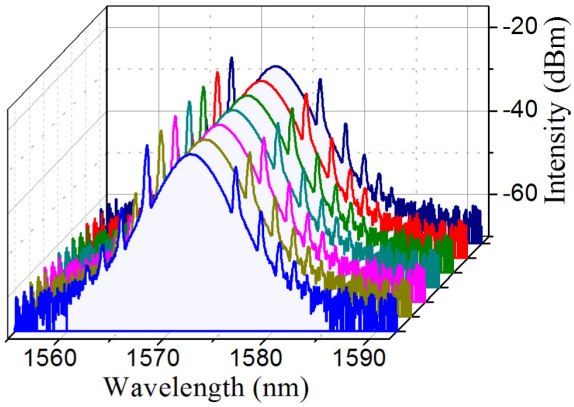

Fig. 8. Long term stability of the output spectra measured under different time.

To investigate the long-term stability of the single soliton operation, we recorded the output spectra every hour over 6 hours under fixed experimental condition, such as pump power of 90 mW, as shown in Fig. 8. Neither the central wavelength drift nor new wavelength component was observed during the measurement, showing excellent repeatability and long term stability.

At last, we also investigated the fiber laser operation without the incorporation of a BP-SA. Even when the pump strength and cavity polarization were tuned in a wide range, only CW state could be observed. It clearly verifies the effectiveness of the BP as a pulse-generator.

#235000 - $15.00 USD Received 23 Feb 2015; revised 25 Apr 2015; accepted 27 Apr 2015; published 7 May 2015

5. Discussions

Enlightened by the narrow direct band-gap properties of bulk BPs (0. 3 ev), it is anticipated that BPs might operate as a broadband saturable absorber even in the mid-IR wavelength regime. Given that the mechanical exfoliation could only produce large size, multi-layered BPs (with thickness larger than 10 layers), which possesses similar electronic band property as the bulk BPs, the as-fabricated multi-layer BP-SAs are not only able to operate at the telecommunication band but also at long wavelength band. Hence, in the future it is interesting to fabricate few-layer BPs (with layer number from mono- up to five-layer) based SAs that could show the thickness dependent band-gap properties. However, it remains challenging to mechanically exfoliate BPs with high throughput, large size, desired thickness and controlled band-gaps. But high yield liquid exfoliation method might be more suitable to fulfill these expectations [42]. In theory, few-layer BP based SAs might operate within certain bandwidth but with tunable and strong optical resonance due to the direct and moderate band-gaps for different layers of BPs. Furthermore, long-term stability and the damage threshold remain a critical problem for the applications of BPs towards the high power regime. This is because of the fragile atomic binding force and the strong activity of phosphorus atoms in contrast with carbon atoms [43,44]. In order to overcome these problems, we expect that the introduction of BPs with other structures, such as organic polymer (which can protect the oxidation from the air/water) and optical wave-guide structures (by depositing BPs onto the surface of D-shape fiber in order to increase the light propagation distance through the lateral interaction scheme) might mitigate the drawbacks of optical damage. Generally speaking, there are plenty of chance to explore the optical properties and applications of BP-related materials, which might highlight the emergence of another new type of 2D optoelectronic materials with direct and tunable semiconducting band-gap that does not own by either graphene or few-layer MoS_2. It therefore offers another choice of candidate 2D materials for some practical device applications at long-wavelength regime, such as mode-locker, Q-switcher, optical modulator, and broadband light processor *etc*.

6. Conclusions

We have demonstrated that BP can be developed as an effective SA for the ultra-fast laser photonics. BP-SAs were prepared by a simple mechanical exfoliation method. We investigated the saturable absorption through the balanced synchronous twin-detector measurement technology and verified that BP has indeed obvious saturable absorption. Depending on the thickness of the BP used, the BP-based SAs either with a modulation depth of 18.55% and saturation intensity 10.74 MW/cm^2 or a modulation depth of 8.1% and saturation intensity of 6.55 MW/cm^2 has been developed. Both the passive Q-switching and the mode-locking operation of the erbium-doped fiber lasers with the BP-SA had been experimentally demonstrated. Our results clearly show that BP could be a new 2D optoelectronic material with potential applications in IR or even mid-IR devices.

Acknowledgments

This work is partially supported by the National 973 Program of China (Grant No. 2012CB315701), the National Natural Science Foundation of China (Grant Nos. 61222505 and 61435010), and Hunan Provincial Natural Science Foundation of China (Grant Nos. 12JJ7005 and 13JJ1012).

#235000 - $15.00 USD Received 23 Feb 2015; revised 25 Apr 2015; accepted 27 Apr 2015; published 7 May 2015